SELECTIVE LEACHING OF ELECTRONIC WASTE FOR VALUABLE METAL RECOVERY BASED ON PARTICLE SIZE

Yidong Xia – Idaho National Laboratory, Idaho Falls, ID, USA
Zachary Diermyer – Idaho National Laboratory, Idaho Falls, ID, USA
Ling Ding – Idaho National Laboratory, Idaho Falls, ID, USA
Noah Berglund – Idaho National Laboratory, Idaho Falls, ID, USA
Jordan Klinger – Idaho National Laboratory, Idaho Falls, ID, USA
Vicki Thompson – Idaho National Laboratory, Idaho Falls, ID, USA
Jiaoyan Li – University at Buffalo, Buffalo, NY, USA
Samuel Forrest – Clemson University, Clemson, SC, USA
Shannon Alford – Clemson University, Clemson, SC, USA

Corresponding author: Yidong Xia (yidong.xia@inl.gov); Tel: +1-208-526-7490

Abstract

Electronic waste (e-waste) recycling for recovery of valuable metals reduces the need for extracting virgin ores and extending the life of the resources. Hydrometallurgical recovery of valuable metals from e-waste, e.g., printed circuit boards (PCBs), is widely used by industry and consists of at least leaching and recovery. Mechanical size reduction (milling) of e-waste after disassembly/sorting is essential before leaching to facilitate liberation and dissolution of valuable metals in the leachate. The methods that the recycling industry currently uses to improve leaching efficiency include leaching the streams of e-waste containing similar compositions, e.g., only CPUs or GPUs. However, this ignores the abundant e-waste mixture in the U.S. and particle size variability in milled e-waste has been underexplored. For example, larger particles (e.g., > 1 mm) contain primarily base metals such as Al and Cu, making it uneconomical to leach them with smaller particles (e.g., < 0.5 mm), which have a much higher mass concentration of valuable metals. If particle size can be used as a key performance indicator to identify particles that potentially have a high mass content of valuable metals and a low mass content of base metals, there will be an opportunity to optimize the leachate for leaching only select particles based on size and scale-up the throughput for leaching. Therefore, this study proposes investigating the feasibility of selective leaching based on the size of milled e-waste particles. To begin with, a two-step milling method is introduced for preparing leaching-ready PCB feedstock with a shredder for coarse milling and a cryogenic mill for fine milling. The cryogenic mill uses a novel configuration for retention of fines and any hazardous airborne materials, and calibration of processing parameters, achieving high mass retention. The milled particles are then separated in size-classified samples (e.g., 4, 2.36, 1, 0.425, 0.25, 0.106, and 0.045 mm) and analyzed using the scanning electron microscopy (SEM) coupled with energy dispersive X-ray spectroscopy (EDS) to determine the mass distribution of valuable metals over size class. Finally, inductively coupled plasma (ICP) spectroscopy analysis is used to detect target metal elements and cross-examine the SEM-EDS results. The potential correlation between ICP and EDS test data in relation to particle size is critical for leaching process optimization.

Introduction and Motivation

E-waste refers to discarded electrical and electronic equipment that is at the end of its economic life span (**Işıldar et al., 2018**). Driven by a rapidly increasing demand for electronic devices and their frequent replacement, e-waste is now the fastest-growing waste stream globally (**Forti et al., 2020**). The benefits of e-waste recycling manifest in its potential to reduce the extraction of virgin ores and extend the life of exhaustible geological resources (**Reck & Graedel, 2012**). Efficient recovery of valuable metals from e-waste is crucial not only for economic reasons but also will reduce the environmental impact of mining virgin ores and to move toward a more sustainable, circular economy.

Printed circuit boards (PCBs) are central constituents in nearly all e-waste and have received much attention due to their high concentrations of copper, precious metals, and other valuable metals, which account for roughly 80% of the intrinsic value of e-waste (**Meskers et al., 2009**). The complex mixture of layered metallic and non-metallic materials in PCBs has presented a unique challenge to the recycling process (**Hao et al., 2020**). Several recycling methods have

been developed to overcome this issue and can be broadly classified as either thermal, involving the addition of heat, such as in pyrolysis or pyrometallugy, or nonthermal, involving mechanical or chemical processing (**Li et al., 2004**). Waste processed by nonthermal methods will often undergo a hydrometallurgical chemical treatment, which has come into focus due to its reduced hazardous gas emissions, relatively low capital costs, and low energy requirements (**Sethurajan et al., 2019**). The main principle of hydrometallurgy is to immerse PCBs in acidic or alkaline solutions to separate valuable metals. This process is referred to as leaching. Then the desired metals are selectively recovered from the leachate. The recovery rate is determined by several process parameters and material attributes, including particle size, which is controlled by the mechanical pretreatment of waste PCBs that involves dismantling, physical separation, and size reduction (**Sethurajan et al., 2019**). Leaching achieves greater dissolution of metals with decreasing feedstock particle size, due to increased total surface area and proportion of metals exposed to the leachate (**Birloaga et al., 2013**). The mechanical pretreatment provides essential liberation and separation of materials, making it indispensable for PCB recycling. The motivation of this work is to address the existing efficiency issues in the current mechanical size reduction methods and suggest potential improvement via novel approaches and analyses.

Review of Related Work

Multiple steps are often required in the comminution (mechanical size reduction) of waste PCB to reach the desired particle size (**Abbadi et al., 2024**). Two-step crushing involving shredding and grinding demonstrated effective metal liberation of waste PCBs (**Oliveira et al., 2010**). Despite their wide adoption, these methods generate excessive fine particles (**Van Eygen et al., 2016**), causing loss of a significant portion of critical elements in output streams (e.g., shredding dusts), resulting in an overall reduction of recycling efficiency (**Marra et al., 2018**). Advanced methods like cryogenic milling (cryo-milling), a processing technique where particulate material is cooled with a cryogenic liquid while being milled to result in particle size reduction toward a minimum value at extended milling times, has been suggested to improve pretreatment (**DeCastro & Mitchell, 2002**). Cooling the mill chamber also helps reduce wear and damage to the equipment (**Daborn & Derry, 1988**). **Suponik et al., 2021** showed cooling waste PCB to cryogenic temperature prior to knife milling significantly improves size reduction efficiency and generated fewer fine particles compared to ambient temperature crushing. Their study, however, used disassembled PCB components before milling and did not sustain cooling during milling. A custom, bench scale cryo-mill using a single steel ball and single PCB part from a computer mouse was shown to reduce the different classes of materials (metal, oxide, and polymer) in the PCB to nanoscale powders in about 1–3 hours, providing complete material liberation (**Tiwary et al., 2017**). The viability of larger-scale cryo-milling for waste PCB yet requires detailed analyses of batch PCB size reduction with extended milling times and the element compositions versus milled particle size distributions.

PCB compositions vary widely based on age, origin, and manufacturer (**Marques et al., 2013**), thus knowing exact concentrations of different elements in a random assortment of waste PCBs is a priori unknown and makes a targeted leaching approach for recycling specific valuable metals difficult. A general measure of classification is based on gold (Au) content, which is the metal containing the most profit for recycling (**Imre-Lucaci et al., 2017**) and separates PCBs into low (<100 parts per million (ppm)), medium (100–400 ppm), or high (>400 ppm) grades (**Hagelüken, 2006**). However, the minor Au content in low-grade PCBs does not convey information of other valuable materials of interest for recycling the PCBs. **Arshadi et al., 2018** found that copper (Cu), silver (Ag), and tin (Sn) were the most economic metals to recover based on weight percentage in PCBs. Element variability also exists within the milled PCBs based across the particle size range. Metal particles are concentrated in larger mesh sizes during milling, as the comminution process struggles to break them down effectively, resulting in elongated shapes and coarser particles (**Nekouei et al., 2018**). In contrast, the nonmetal content in PCBs is brittle, which is more prevalent in fine fractions (**Otsuki et al., 2019**). This variability is further complicated by the small amounts of valuable metals used in PCBs, causing them to adhere to nonmetallic powder in the comminution process (**Zhou & Qiu, 2010**). Imaging techniques such as scanning electron microscopy coupled with energy dispersive X-ray spectroscopy (SEM-EDS) and digital optical microscopy provided insight into the degree of material liberation after comminution (**Pereira Gonçalves & Otsuki, 2019**). SEM-EDS can rapidly provide valuable element composition information but can have sampling errors. To achieve accurate final assay values, wet spectroscopic methods like inductively coupled plasma (ICP) can be used, with results depending on the extent of leaching recovery into the analysis liquor (**Ogunniyi et al., 2009**).

This study explores the correlation between the element distribution and particle size resulting from a two-step size reduction method (shredding then cryo-milling) for waste PCBs. Low-grade PCBs for testing the method are from a U.S. recycling facility with most components attached to the boards, which is a representative case for assorted low-grade waste PCBs. The cryo-mill is configured to maximize retention of fine particles, with milling time ranging from

1- to 4-hour duration to unveil particle size reduction as a function of milling time. An SEM-EDS process is developed for analysis of the milled PCBs, which are size separated so different size classifications can be analyzed individually with SEM-EDS. An ICP process is developed to cross-examine the SEM-EDS results. None of the previous studies investigated the elemental composition of size-specific particles resulting from milling batch PCBs in controlled cryogenic temperature. As the novelty of this work, the elemental compositions of batch waste PCB are unveiled as a function of particle size resulted from cryo-milling to the best of the authors' knowledge, for the first time.

Technology Approach

A mixture of low-grade PCBs containing various components, shown in **Figure 1a**, were received from an industrial refining and recycling company in a fragmented form. These PCBs are components of low-end computer systems, keyboards, and similar accessories. The "low grade" refers to a low level of precious metals, specifically gold (<100 ppm), as described in the previous section. Other content in the PCBs is uncertain, but it is assumed that a large fraction of the mass is composed of the common elements (e.g. copper, aluminum, and polymer elements such as carbon and oxygen). This study will examine what elements are contained in those PCBs and their distribution across the different size classes after size reduction. The as-received PCBs span a large size range, with 74% of the mass contained in 9 – 36 mm screen size range, shown in **Figure 1b**. This section outlines the two-step size reduction process used to break down and homogenize PCB fragments, followed by the composition analysis methods for the size-reduced particles.

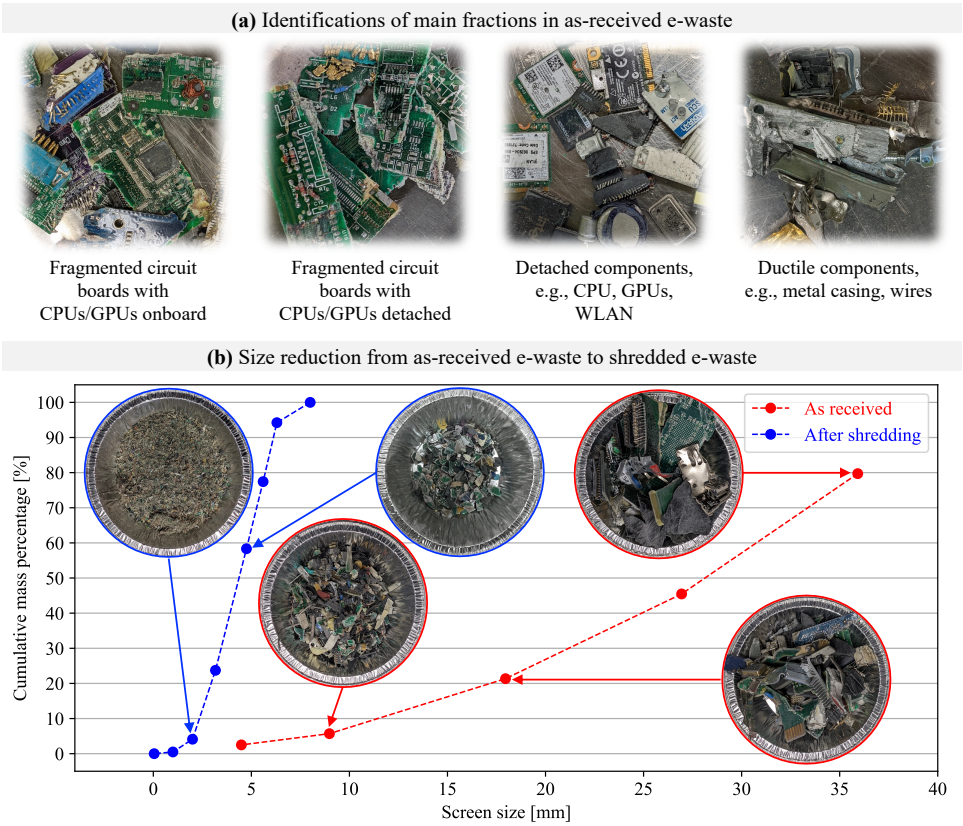

Figure 1: (a) Examples of the received waste PCBs and their typical components. (b) The cumulative mass curves versus sieve screen size for the received PCB fragments (red curve) and after shredding (blue curve).

Two-step size reduction

The PCBs were first size reduced with a Vecoplan VAZ 1100 XL XR rotary shredder (Vecoplan LLC, Trinity, NC, USA), shown in **Figure 2a**. The PCB fragments were fed into the shredder without manual disassembly or removal of components in advance. Though some components were separated from the PCBs by the supplier, shown in **Figure 1a**, they were fed into the shredder with fragmented PCBs, so the elemental composition is not biased by separation. A manual removal of the remaining attached components was not feasible given the heterogeneity of the PCBs. To

minimize the loss of valuable metals through fines and dust during shredding, the use of screen sizes below 4 mm as an empirical estimate should be avoided. The dust generated during shredding is collected from the enclosed shredder system to avoid mass loss during this step. The shredding process was consistent and did not experience any jamming. The shredder reduced all PCB fragments below 8 mm in screen size and reduced 58% of the mass below 4.75 mm, seen in **Figure 1b**. The shredded particles were sieved into 8 size fractions, > 4, 4 – 2.36, 2.36 – 1, 1 – 0.425, 0.425 – 0.25, 0.25 – 0.106, 0.106 – 0.045, and < 0.045 mm (fines), using an RO-TAP RX-29 automatic sieving machine (W.S. Tyler, Mentor, OH, USA). Each size fraction was weighed to obtain a particle size distribution (PSD). Particles were recombined after the PSD measurement and fed into a MTI MSK-SFM-3LN liquid nitrogen cryogenic rotor mill (MTI Corporation, Richmond, CA, USA), referred to as "mill", for further size reduction, shown in **Figure 2b**.

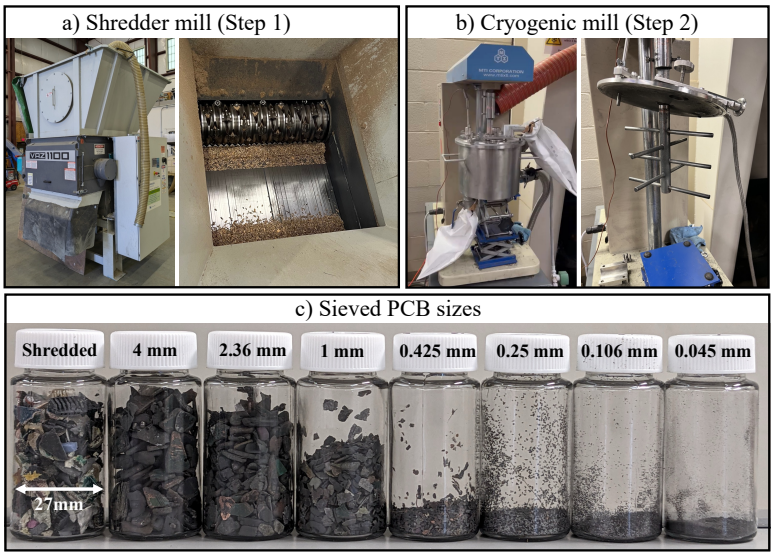

Figure 2: (a) Photos of the shredder seen from the ground view and a top-down view of the cutter blades. (b) The cryogenic mill is pictured fully assembled with white discharge bags attached to the gas outlet ports on top and bottom of the chamber. When the chamber is removed, the lateral agitation bars can be seen connected to a central shaft. (c) After milling, samples are sieved and separated into the eight size classes. Fines are not pictured due to their low total volume, and they are visually indistinguishable from the 0.045 mm size class.

The mill's shaft rotations per minute (RPM) and chamber temperature were kept constant during operation with a control system. The chamber temperature is moderated by injection of liquid nitrogen coolant from a hose attached to the mill chamber. Two ventilation bags are used to enclose, respectively, a material discharge port at the bottom and a gas discharge port on top of the chamber to retain fine particles. The milling media was composed of 4.78 mm diameter 440c stainless steel balls with a total loading mass of 3,020 g placed at the bottom of the chamber. During the trial testing, a suitable shaft RPM of 306 was found, which did not disperse the steel balls into the top ventilation bag. It was also decided that keeping the chamber at 0° C allowed the coolant to need to be injected only intermittently, while mitigating excessive wear and damage to the chamber wall and agitator at a low cost of coolant. In contrast, our trial test showed that keeping the chamber at very low temperature such as -140° C required high coolant injection rate, which resulted in an overflow of liquid/gas in the chamber to weaken the particle collision and displace lots of e-waste particles and steel balls into the top ventilation bag. After each milling test, the milling media was brushed clean to minimize mass loss in this step. Most of the fines were recovered from the two bags and inside the chamber, except a very low loss of mass adhering to the bags. This method guaranteed a mass loss of 6% or below, during the trial. The total recovered mass is weighed then sieved into the eight size fractions described above to obtain the PSD of the milled particles, with a typical example shown in **Figure 2c**. Most of the mass remains in the larger size fractions after milling, indicating that the mechanism of size reduction to smaller particles is mainly via scraping material from the surface of large e-waste fragments, giving them a smoother, grey appearance when compared to the shredded feed.

Composition analysis methods

The milled particle samples were mounted onto stages using copper tape and sputter-coated with gold for 200s at 60 millibar argon pressure. The samples were then imaged using a JEOL-JSM 6610LV SEM. Images were collected at

various magnifications with an accelerating voltage of 10 kV, an objective aperture of 2, a spot size of 40, and a working distance of 10-15 mm. For each size class, multiple samples (n≥3) were analyzed, and multiple images were taken to generate representative and reproducible results. SEM-EDS was used to characterize, localize, and quantify the elements and their distribution in the samples. An EDAX-Ametek EDS detector system and TEAM software were used for the analysis. Mapping analyses were conducted at 150x or 300x magnification with a 30 kV accelerating voltage, an objective aperture of 3, a spot size of 66-80, a dwell time of 200s, an amplitude time of 12.8, and a working distance of 10 mm. In addition to SEM-EDS, we also explored ICP, though briefly in this study. Three different extraction methods were tested for an ICP element analysis to determine the method with largest extraction for each element. The first method was nitric acid wet ashing. 0.5 gram of the milled sample was suspended in 5 mL of 10% nitric acid at 125°C for 1.5 hours on a heat block. Next, the sample was suspended in 3 mL of 30% hydrogen peroxide at 125°C for 1 hour. The temperature of heat block was raised to 200°C. The samples were removed before complete drying occurs and resuspended in 10 mL of 10% nitric acid. Finally, the sample was vigorously shaken and brought to 50 mL with Deionized (DI) water. The second method was crucible furnace ashing and digestion, derived from the sodium peroxide fusion method (**Ogunniyi et al. 2009**). The first step of this method was to place 1 gram of the sample in a crucible heated at 600°C for 1 hour. The remaining sample weight was noted, indicating how much of the sample was non-metallic, but results are based on the initial 1 gram of material. The following steps are the same as the first method, starting from the 5 mL of nitric acid addition. The third method was an aqua regia extraction. 0.5 gram of sample was pre-digested at room temperature for 16 hours with 20 ml of nitric acid and hydrochloric acid HNO_3: HCL (3:1 ratio) mixture. The suspension digested at 130°C for 2 hours on a heat block. Then the sample was diluted to 50 mL with DI water. The final step in this method was a filtering through ashless Whatman filter paper.

Discussion

This section reports the results of the described two-step size reduction method, beginning with a parametric study of the influence of milling time on the PSD of the milled particles. The compositions analyzed with SEM-EDS are then presented to elucidate the valuable metal content versus PSD. The elements with the largest weight percentages in the samples, as indicated by EDS, are then examined with an ICP analysis.

Effects of milling time

The cryo-milling duration of 1, 2, and 4 hours, respectively, was tested at the chamber temperature of 0° C, with each duration repeated with three runs. All the runs resulted in losses of <1% of the feed mass – a nearly complete retention of mass. The three PSD profiles for each duration were averaged and plotted in **Figure 3a**. Different samples of the shredded particles exhibit almost the same PSD, indicating homogeneous feed samples. **Figure 3a** also shows that increased milling time decreases the mass fraction of particles in the larger size range and reduces the overall PSD of the particles. The PSD data in **Figure 3a** are fit using a non-linear least squares (NLLS) method and an accurate model is obtained for all PSDs by fitting the data with the model function

$$\mathrm{m} = \mathrm{a} - \mathrm{e}^{\mathrm{bx}-\mathrm{c}} \tag{1}$$

where a, b, and c are three fitting coefficients, x is the particle size, and m is the cumulative mass. The resultant fitting curves are plotted in **Figure 3b**. Because the three PSD curves of the shredded feed almost coincide, we averaged the data and produced a single fitting curve (dashed black line) in **Figure 3b**. To measure the size reduction simplistically, particle sizes are calculated from the fitting functions for the 50% to 90% cumulative masses in the 10% increments, corresponding to the D50 to D90 characteristic particle sizes. Normalized size reduction is then calculated with the PSD of shredded feed as baseline and plotted in **Figure 3c**. The D50 size reduction, for example, is calculated as

$$\text{Reduced size}_{\mathrm{D50}} = \frac{\mathrm{D50}_{\mathrm{milled}}}{\mathrm{D50}_{\mathrm{shredded}}} * 100 \tag{2}$$

where $\mathrm{D50}_{\mathrm{milled}}$ is the D50 size of cryo-milled particles, $\mathrm{D50}_{\mathrm{shredded}}$ the D50 size of feed shredded particles, and $\text{Reduced size}_{\mathrm{D50}}$ the size reduction percentage. Shown in **Figure 3c**, all characteristic sizes decrease with increasing milling time, and the overall PSD are reduced. The percentage reduction increases for smaller particle sizes, e.g., D90 vs. D50. Some specific percentages are given in the plot to show the difference. For example, D90 decreases by 43% in the first hour of milling, whereas D50 decreases by only 11%. The outcome shows that extending milling time leads to increased mass in smaller particles. It is also found that size reduction is less effective given more milling time, as

D90 and D50 are reduced by only 2% and 3%, respectively, when milling time is increased from 2 to 4 hours, shown in **Figure 3c**. Milling the shredded PCBs more than 2 hours is therefore not necessary from the economic perspective.

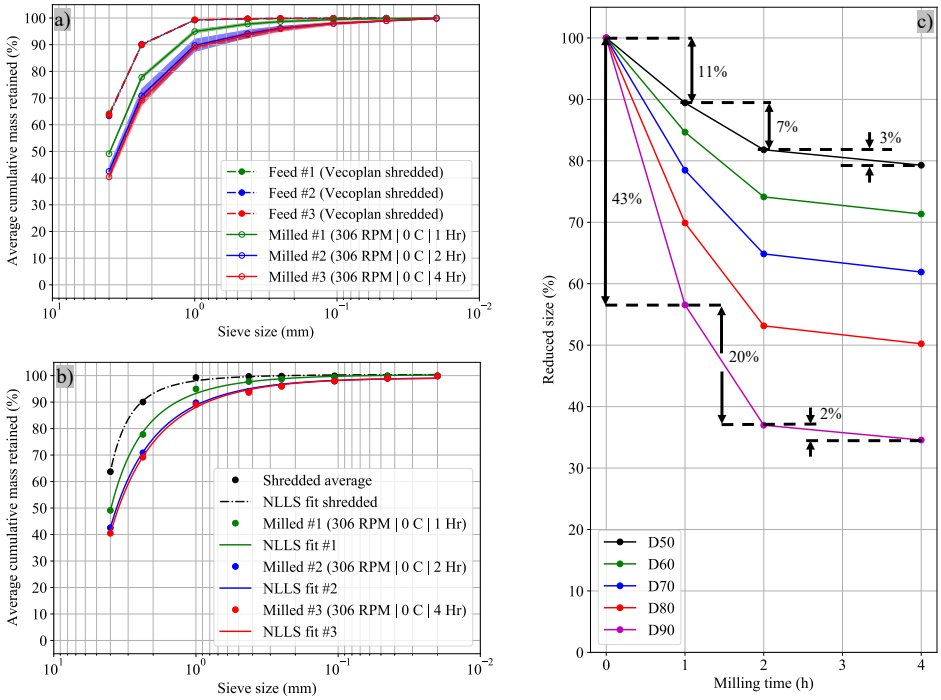

Figure 3: (a) Average PSDs are shown with dashed lines for the shredded feed and solid lines for milled particles. The shaded area is the uncertainty range of the milled PSDs. Green, blue, and red data points represent the PSDs of 1-, 2-, and 4-hour milling durations. (b) Average milled PSD data points fit by the solid lines. Green, blue, and red lines correspond to the fits of 1-, 2-, and 4-hour PSD data, respectively. (c) Reduced size percentage of the D50 to D90 particle sizes with respect to the shredded feed versus milling time.

Element variability

To learn the content and variability of elements in low-grade PCBs, the described SEM-EDS analysis was performed for the milled particles in each size group. The SEM-EDS scans reveal many of the surface morphologies after milling, as shown in **Figure 4a-f**. The results were separated into the base and valuable metal elements with the largest percent weight. Though the base metal and non-metal elements are not of high interest for PCB recycling, they account for a large fraction of total weight and were analyzed for completeness. These elements are constituents of polymers (carbon (C), oxygen (O)), ceramics (calcium (Ca), O), fiberglass bases (silicon (Si), O), or structural components like steel (iron (Fe)) in the PCBs. An SEM image of the 0.045 mm fine particles in **Figure 4a** shows high aspect ratio particle shapes, and the pairing analysis with EDS in **Figure 4b**, reveal that the structures are composed of silicon and originate from the fiberglass base of the PCBs, which broke off into tiny pieces during milling. The EDS results indicate as much as 66% of the PCB sample at sub-mm sizes belongs to base metal and non-metal elements, mainly C, O, Si, Ca, and Fe, shown in **Figure 4g**. Other base metal and non-metal elements are included in the EDS scan, shown in the table at the top of **Figure 4**, which are though not plotted because of their relatively low weight percentage.

Valuable metals are desired targets of PCB recycling based on a list of special metals (**Chancerel et al., 2009**) and the elements in the U.S. Geological Survey final list of critical minerals (**U.S. Geological Survey, 2022**). An SEM image of the > 4 mm size fraction is shown in **Figure 4c**. The EDS scan of this size fraction includes metallic structures such as tin (Sn) from the PCB solder connections, copper (Cu) from the conducting layer, and aluminum (Al) from attached components, shown in **Figure 4d-f**, respectively. The valuable metals with the largest weight percentage in the sample are beryllium (Be), Al, Cu, barium (Ba), and Sn, shown in **Figure 4h**. Some trends can be observed in the plot which correlate with the material properties of the metals. For example, ductile metals such as Cu and Al are more abundant at larger particle sizes, whereas brittle elements like Be are more concentrated at smaller particle sizes. A remarkable finding from **Figure 4h** lies in the significantly larger amount of Be at smaller particle sizes than other valuable metals. One explanation for this finding is the use of Be as an alloying element in the Cu conductors of PCBs,

which is a commonly used method to improve the thermal properties of Cu (**Luda, 2011**). Cu and Al are detected at significant levels relative to the other valuable metals, consistent with **Marra et al., 2018**. The other valuable elements included in the EDS scan are only listed in the top table in **Figure 4**, but not plotted because of their low content.

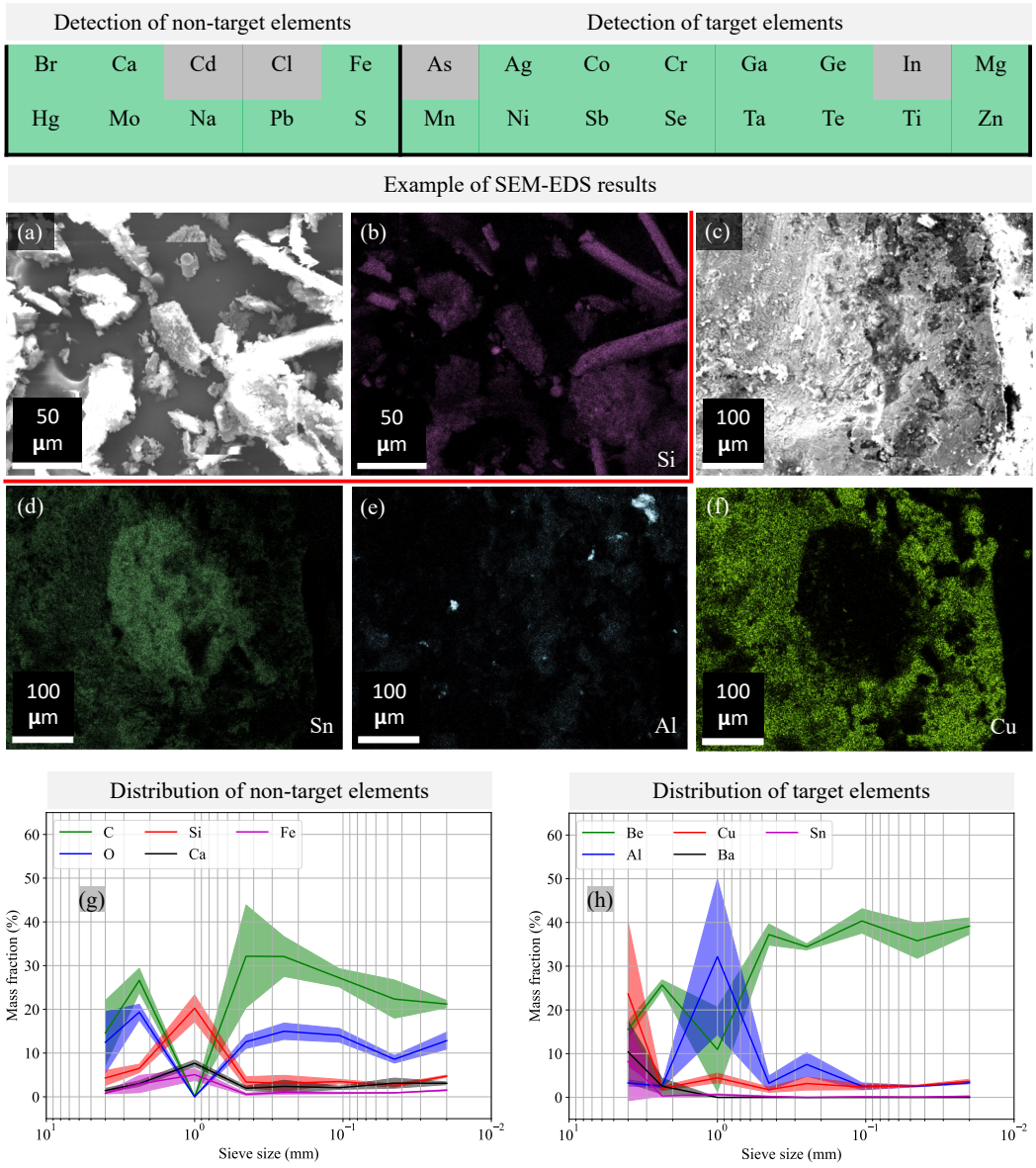

Figure 4: SEM-EDS element detection is shown in the table at the top of the image in green (detected) and grey (not detected). An SEM image (a) and the corresponding EDS scan (b) of the fine particles show large aspect ratio silicon structures, while an SEM image (c) and EDS scan of the largest particles exhibit metallic elements, such as tin (d), aluminum fragments (e), and copper (f). Base metal and non-metal element mass fractions (g) and select valuable element mass fractions (h) are plotted with shaded regions showing the error percentage.

Beryllium, Barium, and Tin recovery with ICP

The described three ICP analysis methods were used to cross examine the milled samples. Each method was repeated 3 times to obtain the average results, which are listed in part 1 of **Table 1**. Since ICP must be targeted to search for individual elements, a selection of three valuable metal elements (Be, Ba, and Sn) found from SEM-EDS were used. These elements had the largest detected weight percent among valuable elements in the sample other than Cu and Al. Because Cu and Al are commonly used in PCBs and their presence is expected, no further testing is needed. The ICP

results in part 1 of **Table 1** were based on the 0.045 mm size class as an initial investigation into the small size groups to provide insights into the quantity of valuable metals in fine particles. The results did not show any Be but confirmed Ba and Sn. It is speculated that the non-detection of Be in ICP is potentially due to sampling error between SEM-EDS and ICP, which requires further investigation for explanation. The extractability of Ba, Be, and Sn across the particle sizes used the aqua regia method, as it had a similar extraction of Ba to the routine digest method but significantly more for Sn (532 ppm with routine digest vs. 23370 ppm with aqua regia). This is consistent with **Ogunniyi et al., 2009** and **Holgersson et al., 2018**, where aqua regia has commonly been used to digest Ba, Be, and Sn from PCBs. Part 2 of **Table 1** shows the detectable distribution of Be, Ba, and Sn at each particle size and milling time. For sizes over 0.25 mm, the variability of Ba and Sn increases greatly, indicating that the milled PCB particles are homogeneous only at sub-mm sizes. Also, there is not a huge difference in the trends of Ba and Sn with different durations of milling time. Among the ICP test samples, Be was eventually detected in the particles of smallest sizes with the 1- and 4-hour milling durations and at very low levels of concentration.

Sn has a large concentration at all particle sizes, which can be attributed to the ubiquitous use of Sn in solder joints. Because of the ductile nature of solder, it can remain bonded to large particles after milling. The use of solder on PCB surfaces allows some to be removed by attrition and become mixed into smaller particles. A maximum average Sn concentration is found in the 0.425 mm size class for all the tested durations of milling time. Ba content increases with increasing particle size, due to its use in ceramic capacitors, which are brittle and can easily break during milling, as mentioned in **Li et al., 2004**. The detected amounts of Sn and Ba at all particle sizes are consistent with **Ogunniyi et al., 2009** and **Holgersson et al., 2018**, where 29,000-35,000 ppm of Sn and 1,700-8,100 ppm of Ba were reported.

Table 1: List of the ICP test results for the select valuable metal elements.

Part 1: Comparison of ICP results using three digestion methods for detection of select valuable elements. The reported values are an average of three repeated tests on the 0.045 mm size fraction of the milled samples.			
Element	**Routine digest (ppm)**	**Dry + wet ash (ppm)**	**Aqua regia (ppm)**
Ba	12881 ± 560	12743 ± 512	11851 ± 407
Be	0.0	0.0	0.0
Sn	532 ± 58	859 ± 69	23370 ± 593
Part 2: the results of ppm vs. size and milling time below were obtained using aqua regia digestion.			
Ba	**1-hour milling (ppm)**	**2-hour milling (ppm)**	**4-hour milling (ppm)**
4.000 mm	443 ± 144	329 ± 139	303 ± 112
2.360 mm	240 ± 83	492 ± 92	706 ± 384
1.000 mm	454 ± 162	603 ± 18	518 ± 112
0.425 mm	1051 ± 548	2622 ± 2146	982 ± 349
0.250 mm	3036 ± 432	4030 ± 809	3101 ± 352
0.106 mm	4057 ± 36	3992 ± 560	3794 ± 293
0.045 mm	7135 ± 531	11851 ± 407	5832 ± 368
Sn	**1-hour milling (ppm)**	**2-hour milling (ppm)**	**4-hour milling (ppm)**
4.000 mm	29608 ± 26647	28226 ± 25403	38959 ± 24499
2.360 mm	4569 ± 3922	7813 ± 3782	15700 ± 10547
1.000 mm	3888 ± 1485	63299 ± 26248	7541 ± 3556
0.425 mm	43723 ± 8311	64577 ± 16544	30403 ± 11164
0.250 mm	23403 ± 1956	22096 ± 2653	19666 ± 431
0.106 mm	17203 ± 115	14143 ± 1176	20355 ± 177
0.045 mm	21032 ± 332	23370 ± 593	26845 ± 647
Be	**1-hour milling (ppm)**	**2-hour milling (ppm)**	**4-hour milling (ppm)**
0.106 mm	0.13 ± 0.05	0.0	0.20 ± 0.00
0.045 mm	0.49 ± 0.14	0.0	0.79 ± 0.08

Conclusions

A two-step mechanical size reduction method was introduced to process waste PCBs for hydrometallurgical recovery of valuable materials. The relationships between valuable metal content, particle size, and milling time were analyzed. Element variability in the size classified samples was explored using SEM-EDS, followed by ICP analysis for targeted elements. The major findings are as follows. First, the devised mill configuration has achieved a nearly complete mass

retention, allowing a comprehensive element analysis of all size classes, including fine particles below 50 um. Second, SEM-EDS analyses showed that up to 66% of milled PCB samples at sub-mm sizes belongs to base metal and non-metal elements; the content of valuable metals varies based on particle size, with particles above 1 mm containing most of copper and aluminum, while smaller sub-mm particles contain more valuable metals such as beryllium. Third, the ICP analyses showed nearly nonexistence of beryllium in the 45-um size class but confirmed the existence of barium and tin. One explanation is due to possible sampling error, warranting future research. Fourth, optimal milling duration for shredded PCBs would be 2 hours or less in this study. For barium recovery, it is beneficial to use smaller particles for higher concentrations. For tin recovery, particle size around 500 um shows the highest concentration.

Acknowledgements

The research was supported by the Idaho National Laboratory (INL) Laboratory Directed Research & Development (LDRD) Program under U.S. Department of Energy Idaho Operations Office Contract DE-AC07-05ID14517.

References

Abbadi, A., Rácz, Á., Bokányi, L., Exploring the comminution process of waste printed circuit boards in recycling: a review. J. Mater. Cycles Waste Manag., 1-23, 2024.

Arshadi, M., Yaghmaei, S., Mousavi, S. M., Content evaluation of different waste PCBs to enhance basic metals recycling. Resour. Conserv. Recycl., 139, 298-306, 2018.

Birloaga, I., De Michelis, I., Ferella, F., Buzatu, M., Vegliò, F., Study on the influence of various factors in the hydrometallurgical processing of waste printed circuit boards for copper and gold recovery. Waste Manag., 33(4), 935-941, 2013.

Chancerel, P., Meskers, C. E., Hagelüken, C., Rotter, V. S., Assessment of precious metal flows during preprocessing of waste electrical and electronic equipment. J. Ind. Ecol., 13(5), 791-810, 2009.

Daborn, G. R. and Derry, R., Cryogenic comminution in scrap recycling. Resour. Conserv. Recycl., 1(1), 49-63, 1988.

DeCastro, C. L. and Mitchell, B. S., Nanoparticles from mechanical attrition. Synthesis, functionalization, and surface treatment of nanoparticles, pp.1-14, American Scientific Publishers, 2002.

Forti, V., Balde, C. P., Kuehr, R., Bel, G., The Global E-waste Monitor 2020: Quantities, flows and the circular economy potential, pp.1-120, United Nations University/United Nations Institute for Training and Research, International Telecommunication Union, and International Solid Waste Association 2020.

Hagelüken, C., Recycling of electronic scrap at Umicore's integrated metals smelter and refinery. Erzmetall, 59(3), 152-161, 2006.

Hao, J., Wang, Y., Wu, Y., Guo, F., Metal recovery from waste printed circuit boards: A review for current status and perspectives. Resour. Conserv. Recycl., 157, 104787, 2020.

Holgersson, S., Steenari, B. M., Björkman, M., Cullbrand, K., Analysis of the metal content of small-size Waste Electric and Electronic Equipment (WEEE) printed circuit boards—part 1: Internet routers, mobile phones and smartphones. Resour. Conserv. Recycl., 133, 300-308, 2018.

Imre-Lucaci, Á., Nagy, M., Imre-Lucaci, F., Fogarasi, S., Technical and environmental assessment of gold recovery from secondary streams obtained in the processing of waste printed circuit boards. Chem. Eng. J., 309, 655-662, 2017.

Işıldar, A., Rene, E. R., van Hullebusch, E. D., Lens, P. N., Electronic waste as a secondary source of critical metals: Management and recovery technologies. Resour. Conserv. Recycl., 135, 296-312, 2018.

Li, J., Shrivastava, P., Gao, Z., & Zhang, H. C., Printed circuit board recycling: a state-of-the-art survey. IEEE transactions on electronics packaging manufacturing., 27(1), 33-42, 2004.

Luda, M. P., Recycling of printed circuit boards, pp.285-298, IntechOpen, 2011.

Marques, A. C., Cabrera, J. M., de Fraga Malfatti, C., Printed circuit boards: a review on the perspective of sustainability. J. Environ. Manag., 131, 298-306, 2013.

Marra, A., Cesaro, A., Belgiorno, V., Separation efficiency of valuable and critical metals in WEEE mechanical treatments. J. Clean. Prod., 186, 490-498, 2018.

Meskers, C. E. M., Hagelüken, C., Salhofer, S., Spitzbart, M., Impact of pre-processing routes on precious metal recovery from PCs, pp.527-540, Proceedings of EMC Vol. 2, 2009.

Nekouei, R. K., Pahlevani, F., Rajarao, R., Golmohammadzadeh, R., Sahajwalla, V., Two-step pre-processing enrichment of waste printed circuit boards: Mechanical milling and physical separation. J. Clean. Prod., 184, 1113-1124, 2018.

Ogunniyi, I. O., Vermaak, M. K. G., Groot, D. R., Chemical composition and liberation characterization of printed circuit board comminution fines for beneficiation investigations. Waste Manag., 29(7), 2140-2146, 2009.

Oliveira, P. C., Cabral, M., Nogueira, C. A., Margarido, F., Printed circuit boards recycling: Characterization of granulometric fractions from shredding process, pp.1434-1439, Materials Science Forum, Vol. 636, Trans Tech Publications Ltd., 2010.

Otsuki, A., Pereira Gonçalves, P., Leroy, E., Selective milling and elemental assay of printed circuit board particles for their recycling purpose. Metals, 9(8), 899, 2019.

Pereira Gonçalves, P. and Otsuki, A., Determination of liberation degree of mechanically processed waste printed circuit boards by using the digital microscope and SEM-EDS analysis. Electronics, 8(10), 1202, 2019.

Reck, B. K. and Graedel, T. E., Challenges in metal recycling. Science, 337(6095), 690-695, 2012.

Sethurajan, M., van Hullebusch, E. D., et al, Recent advances on hydrometallurgical recovery of critical and precious elements from end of life electronic wastes—a review. Crit. Rev. Environ. Sci. Technol., 49(3), 212-275, 2019.

Suponik, T., Franke, D. M., Nuckowski, P. M., Matusiak, P., Kowol, D., Tora, B., Impact of grinding of printed circuit boards on the efficiency of metal recovery by means of electrostatic separation. Minerals, 11(3), 281, 2021.

Tiwary, C. S., Kishore, S., Vasireddi, R., Mahapatra, D. R., Ajayan, P. M., Chattopadhyay, K., Electronic waste recycling via cryo-milling and nanoparticle beneficiation. Materials Today, 20(2), 67-73, 2017.

US Geological Survey., 2022 Final list of critical minerals. Federal Register, 87(37), 2022.

Van Eygen, E., De Meester, S., Tran, H. P., Dewulf, J., Resource savings by urban mining: The case of desktop and laptop computers in Belgium. Resour. Conserv. Recycl., 107, 53-64, 2016.

Zhou, Y., Qiu, K., A new technology for recycling materials from waste printed circuit boards. J. Hazard. Mater., 175(1-3), 823-828, 2010.

About the Authors

Yidong Xia, Ph.D., is a senior research scientist in Idaho National Laboratory's Engineering Process Design & Realization Department. Dr. Xia's research fields include geosciences and microfluidics, renewable carbon resources, and waste sources recycling, and manufacturing. Dr. Xia is the presenter of the content at the conference.

Zachary Diermyer is a student intern at Idaho National Laboratory and Ph.D. candidate at the State University of New York at Buffalo. Mr. Diermyer's work focuses on multiscale/multiphase flow physics and industrial applications.

Ling Ding, Ph.D., is a research engineer in Idaho National Laboratory's Department of Bioenergy Feedstocks Technology. Dr. Ding's research fields include feedstock variabilities in renewable carbon resources and waste.

Noah Berglund is a research engineer in Idaho National Laboratory's Bioenergy Feedstocks Technology Department. Mr. Berglund is specialized in experimental design, instrumentation, and testing of sophisticated energy systems.

Jordan Klinger, Ph.D., is a senior research engineer in Idaho National Laboratory's Bioenergy Feedstocks Technology Department. Dr. Klinger's research fields include feedstock mechanical and thermal processing methods.

Vicki Thompson, Ph.D., is a distinguished research scientist and manager for Idaho National Laboratory's Bioenergy Feedstocks Technology Department. Dr. Thompson's research fields include renewable feedstocks and processing.

Jiaoyan Li, Ph.D., is an assistant professor of mechanical engineering at the State University of New York at Buffalo. Dr. Li's research focuses on multiscale material modeling, multi-physics coupling, and micro-continuum theories.

Samuel Forrest, Ph.D., is a Research Associate of the Agricultural Service Lab at Clemson University. Dr. Forrest completed postdoctoral work and attained a PhD in Genetics at Clemson University. Dr. Forrest has nearly a decade of chemical safety-related experience from his previous role at the Clemson Research Safety office.

Shannon Alford, Ph.D., is the Director of Analytical Laboratories for Regulatory Services at Clemson University. Dr. Alford completed postdoctoral work and PhD (Biochemistry) at Virginia Tech, MS (Analytical Chemistry) from Mississippi State University, and BS (Chemistry) from Clemson University.